

Scaling properties of driven interfaces: Symmetries, conservation laws, and the role of constraints

Z. Rácz,* M. Siegert, D. Liu, and M. Plischke

Physics Department, Simon Fraser University, Burnaby, British Columbia, Canada V5A 1S6

(Received 11 December 1990)

One-dimensional models of surface dynamics are studied analytically and by numerical simulation. In all cases the number of particles that form the deposit is conserved. We find that an initially flat surface, in general, roughens as a function of time and can be characterized by a width ξ which obeys the scaling form $\xi(L, t) = L^\chi f(t/L^z)$ for a deposit on a substrate of linear dimension L . Restricted solid-on-solid (RSOS) -type models in which the microscopic dynamics obeys detailed balance are shown to be in the “free-field” universality class with exponents $z = 4$ and $\chi = \frac{1}{2}$. On the other hand, if detailed balance is broken, several universality classes exist. As the “maximum-height-difference” constraint in a RSOS model is varied, one can observe a phase transition between a flat phase ($z = 2, \chi = 0$) and a grooved phase characterized by a steady-state exponent $\chi = 1$ but with no scaling in the relaxation process. At the transition point, a nontrivially rough surface emerges with exponents ($z \approx 3.67, \chi \approx 0.33$) close to those of the conserved Kardar-Parisi-Zhang equation. We propose a phenomenological model that may account for these observations.

I. INTRODUCTION

The origin of dynamic scaling and the identification of universality classes in nonequilibrium growth and deposition processes have been extensively discussed in the literature.¹⁻¹⁸ In growth processes such as ballistic deposition and its variants,^{1,4,5,12} or the Eden process,^{2,3,7} an initially smooth interface roughens as the deposit develops. In the case of deposition onto a substrate of linear dimension L , the width of the interface ξ typically obeys scaling and has the form

$$\xi(L, t) = L^\chi f(tL^{-z}), \quad (1)$$

where the steady-state exponent χ and the dynamic exponent z depend on the dimensionality d of the substrate and on the underlying symmetries of the growth process.⁶ The scaling function $f(x)$ has the asymptotic behavior $f(x) \rightarrow \text{const}$ as $x \rightarrow \infty$ and $f(x) \sim x^{\chi/2}$ as $x \rightarrow 0$.

The above scaling form can be derived analytically for a number of growth processes which seem to be well described by the following nonlinear differential equation proposed by Kardar, Parisi, and Zhang¹⁴ (KPZ):

$$\frac{\partial h(\mathbf{x}, t)}{\partial t} = \nu \nabla^2 h(\mathbf{x}, t) + \frac{\lambda}{2} [\nabla h(\mathbf{x}, t)]^2 + \eta(\mathbf{x}, t). \quad (2)$$

Here h is the height of the deposit, ν and λ are parameters, and η is a function representing Gaussian white noise. The important parameter λ is in general nonzero when the number of particles in the deposit grows. When λ is zero, Eq. (2) yields “equilibrium” roughening characterized by free-field exponents ($\chi = \frac{1}{2}$ and $z = 2$ for $d = 1$). For finite λ exact results ($z = \frac{3}{2}, \chi = \frac{1}{2}$) are available only for one-dimensional substrates¹⁴ where the results of simulations^{2,3,6,9} are in excellent agreement with the predictions of the KPZ equation. In a higher dimension we have only the scaling relation¹⁴⁻¹⁵ $z + \chi = 2$. The critical dimension of the KPZ equation is $d_c = 2$, and much

effort¹⁶ has gone into the study of Eq. (2) and of discrete deposition models^{5,7-9,11-13} which may be describable by this equation at the critical dimension.

The similarities between roughening and dynamic critical phenomena naturally led to the question of whether the exponents χ and z are dependent on the conservation laws of the system. With this question in mind, Sun, Guo, and Grant¹⁷ investigated a model of surface reconstruction in which the volume of the deposit is conserved. They studied the following “conserved” variant of the KPZ equation:

$$\frac{\partial h(\mathbf{x}, t)}{\partial t} = -\nabla^2 \left\{ \nu \nabla^2 h(\mathbf{x}, t) + \frac{\lambda}{2} [\nabla h(\mathbf{x}, t)]^2 \right\} + \eta(\mathbf{x}, t) \quad (3)$$

which is assumed to be a model of surface reconstruction driven, not by equilibrium fluctuations, but rather by some external flux (e.g., electric current or heat flux). In order to ensure that the volume of the deposit is conserved, the noise function $\eta(\mathbf{x}, t)$ must be a function that represents conservative white noise, i.e.,

$$\begin{aligned} \langle \eta(\mathbf{x}, t) \rangle &= 0, \\ \langle \eta(\mathbf{x}, t) \eta(\mathbf{x}', t') \rangle &= -\nabla^2 \delta^d(\mathbf{x} - \mathbf{x}') \delta(t - t'). \end{aligned} \quad (4)$$

It has been shown by both renormalization-group methods¹⁷ and by direct integration of the equations¹⁸ that Eqs. (3) and (4) yield a different set of exponents than those of the KPZ equation. The question then arises as to what kinds of processes yield the conserved KPZ equation in the continuum limit.

In Monte Carlo simulations of surface evolution models, blocks or particles of a certain size are added to, moved, or subtracted from the deposit according to certain rules. The connection with a Langevin equation of the form (2) or (3) can then be made through a master

equation,⁶ approximated by its long-wavelength limit. Alternatively, one can make the connection through symmetry arguments by assuming that the continuum limit is described by an equation that obeys the apparent symmetries of the discrete process and that contains the minimal number of relevant¹⁷ (in the renormalization-group sense) terms. Each approach has its inherent difficulties. In the master-equation formalism, one arrives in principle at an infinite hierarchy of equations that must be decoupled. The consequences of such a mean-field decoupling are unknown. In the other approach, there is always the possibility that a hidden symmetry may be missed. Thus, ultimately, the question of equivalence is decided by comparing the exponents obtained in a simulation of the discrete process to those predicted by the continuum equation.

Sun, Guo, and Grant¹⁷ simulated a restricted solid-on-solid model with short-range hopping dynamics and found exponents sufficiently close to those of the conserved KPZ equation to conclude that Eq. (3) is a continuum description of the process. Their model clearly satisfies the particle conservation law inherent in Eq. (3). Closer examination of the model reveals, however, an extra symmetry ($h \rightarrow -h$) that excludes the possibility of a $\nabla^2 (\nabla h)^2$ term in the continuum equation.

Thus the question of what kind of process can be described by the conserved KPZ equation remains open and, in this paper, we present the results of our search for such a process. Our main conclusion is that the breaking of the symmetry $h \rightarrow -h$ through a breaking of detailed balance does not automatically lead to a process describable by Eq. (3). The conserved KZ equation seems to appear in rather exceptional circumstances when a phase transition occurs between a flat phase and a grooved phase.

The structure of this paper is as follows. In Sec. II we describe the discrete models, which we have simulated, and discuss the form of the Langevin equation that might be expected in the long-wavelength limit. Section III contains the results of the simulations and the conclusions drawn from comparison of the numerical results with the solutions of the Langevin equation.

II. MODELS FOR CONSERVED SURFACE DYNAMICS

We investigate a family of models for surface rearrangement that are quite similar to the model of Ref. 17. A one-dimensional substrate of length L (number of adsorption sites) is considered. The surface is characterized by the height of the deposit h_i at site i , and the moving particles are blocks of height Δ that can hop to neighboring sites within a maximum distance, which we generally have taken to be two lattice sites. Since no new particles are introduced, $\langle h \rangle = (\sum_i h_i)/L$ is conserved, and since the maximum hopping distance is a finite number independent of L , the conservation law has a local character.

Particles are selected at random, and a move is permitted if the constraint $|h_i - h_{i+1}| \leq H$ is satisfied for all i at the beginning and at the end of the process. The entire system is subject to periodic boundary conditions. We

have used two different procedures of implementing the dynamics.

(i) Once a particle is selected for a trial move a random number determines whether the particle will be moved to the left or to the right. If the move would result in a violation of the constraint $|h_i - h_{i+1}| \leq H$, the attempted move is abandoned and a new particle is selected. This procedure corresponds¹⁹ to that of Ref. 17.

(ii) If a move to the left (right) is rejected, a move to the right (left) is attempted. If this too is rejected, a new particle is selected for the next attempted move.

At first glance, the two procedures do not seem significantly different, and one might expect that they are related by a simple change of the time scale. A more detailed analysis, presented below, reveals that procedure (i) obeys detailed balance, whereas procedure (ii) does not and, concomitantly, breaks the symmetry $h(x, t) \rightarrow -h(x, t)$. As we also show below, procedure (i) does respect the reflection symmetry $h(x, t) \rightarrow -h(x, t)$ and therefore cannot, in the long-wavelength limit, be modeled by an equation of the form (3). The numerical results presented in Ref. 17, which seemed to be consistent with the renormalization-group predictions for Eq. (3), are in fact due to finite-size effects. The appropriate continuum equation for procedure (i) is Eq. (3) with the coefficient $\lambda=0$. Thus we obtain $z=4$ and $\chi=\frac{1}{2}$. Evidence for this will be presented in Sec. III.

We now discuss the violation of detailed balance by process (ii) for the case $\Delta=H/2$. In Fig. 1 we show three configurations of the surface. Configuration (a) may change into configuration (b) by the hopping of block 2 to the left, or into configuration (c) by the hopping of block 1 to the left. If block 2 is selected for a trial move, the probability $W(a, b)$ of the transition to state (b) is $\frac{1}{2}$ as both a move to the left and to the right are permitted by the rules. On the other hand, if block 1 is selected, the

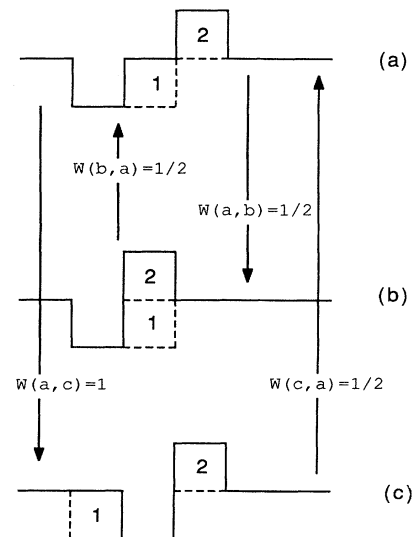


FIG. 1. Illustration of the breakdown of detailed balance for the case of procedure (ii). See text for discussion.

probability $W(a,c)$ of a move to the left is 1 since a move to the right is forbidden by the constraint $|\delta h| \leq H = 2\Delta$.

Let the steady-state probabilities of states (a) , (b) , and (c) be $P(a)$, $P(b)$, and $P(c)$. Since (c) differs from (b) only by a shift of the entire configuration and since we have imposed periodic boundary conditions, we have $P(b) = P(c)$. The relation of $P(a)$ to $P(b)$ is unknown. However, detailed balance requires

$$\begin{aligned} P(a)W(a,b) &= P(b)W(b,a), \\ P(a)W(a,c) &= P(c)W(c,a), \end{aligned} \quad (5)$$

which leads to the condition

$$\frac{W(a,b)}{W(a,c)} = \frac{W(b,a)}{W(c,a)}. \quad (6)$$

As can be seen from Fig. 1, the left-hand side is $\frac{1}{2}$ while the right-hand side is 1, and we conclude that detailed balance is violated. We note that in procedure (i) all transition probabilities $W(i,j)$ between allowed configurations are equal to $\frac{1}{2}$, which means that detailed balance is maintained.

In Fig. 2 we examine the analogous transitions for the reflected configurations ($h_i \rightarrow -h_i$, for all i). Denoting the reflected configuration of (a) by (a') , for example, we see that $W(a',b') \neq W(a,b)$ and $W(a',c') \neq W(a,c)$ for procedure (ii). Conversely, for procedure (i), $W(i',j') = W(i,j)$ for all configurations. Thus we expect that a Langevin equation for process (ii) might contain terms that have even powers of h , but that the corresponding equation for process (i) will quite generally be symmetric under $h(x,t) \rightarrow -h(x,t)$.

We now discuss the form of the continuum equations by which one might model the processes described above.

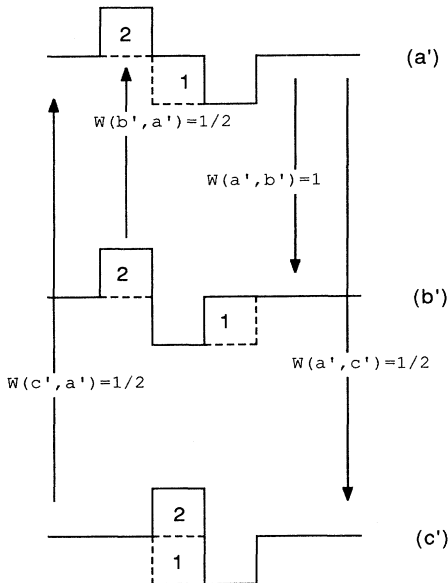


FIG. 2. Illustration of the fact that the dynamics of procedure (ii) break reflection symmetry. See text for discussion.

We begin with a master equation for the discrete process. In the case of a growing surface, we have previously shown⁶ that Eq. (1) can be obtained in a natural way through such considerations.

Figure 3 shows a segment of the surface with spacing ϵ between absorption sites. The height of the surface at point i can change through the addition or removal of a block of height Δ and width ϵ . For simplicity, we consider hopping of blocks only to nearest-neighbor sites. Then the average rate of change of the height at point i will be given by

$$\frac{\tau_0}{\Delta} \frac{\partial \langle h_i(t) \rangle}{\partial t} = \langle W(i-1, i) + W(i+1, i) - W(i, i-1) - W(i, i+1) \rangle, \quad (7)$$

where $W(i,j)$ is the probability of hopping from site i to site j and the average $\langle \dots \rangle$ is over the probability distribution $P(\{h_i\}, t)$, which is the solution of the master equation with the given hopping probabilities $W(i,j)$. In general, the hopping probability $W(i,j)$ depends on the height differences of nearest-neighbor sites and, in the case of procedure (ii), will involve the heights at points $i-2, i-1, i, i+1$, and $i+2$, i.e.,

$$W(i, i+1) = \phi(\sigma_{i-1}, \sigma_i, \sigma_{i+1}, \sigma_{i+2}), \quad (8)$$

with $\sigma_i = (h_i - h_{i-1})/\epsilon$. In the case of procedure (i), there will be no dependence on σ_{i-1} .

Particular realizations of these processes lead to different functional forms for the transition probabilities. Rather than presenting a complete derivation for a specific case, we will argue for a generic form of the continuum equation. The steps in the argument are as follows.

(1) The transition probabilities are expanded in powers of the height differences, i.e., we write

$$\begin{aligned} \phi(\sigma_{i-1}, \sigma_i, \sigma_{i+1}, \sigma_{i+2}) \\ = 1 + \sum_{\alpha} c_{\alpha} \sigma_{i+\alpha} + \sum_{\alpha, \beta} d_{\alpha\beta} \sigma_{i+\alpha} \sigma_{i+\beta} + \dots \end{aligned} \quad (9)$$

(2) A continuous spatial variable $x = i\epsilon$ is introduced, and the discrete-valued function $h_{x+\epsilon}(t)$ is expanded in powers of ϵ . The assumption underlying this step is that a coarse-graining procedure has been carried out, and

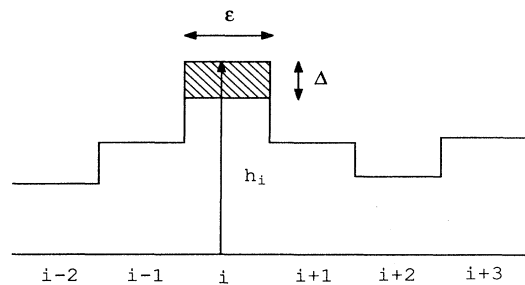


FIG. 3. Possible configuration of a section of the interface. The moving particles are blocks of height Δ and width ϵ .

thus $h(x, t)$ has become a continuous function of x . The implementation of such a coarse-graining procedure is a nontrivial task, and there are few situations for which it has been done with mathematical rigor.²⁰ Thus, in practice, coarse graining is replaced by smoothing out the discreteness of $h(x, t)$. For example, step functions like $\theta(\xi)$ can be replaced by continuous functions like $[1 + \tanh(\xi/a)]/2$, where a is an arbitrary parameter. Since neither the smoothing nor a proper coarse graining changes the symmetry of the equations, we believe that this step does not affect our conclusions regarding the general form of the equation as given below.

(3) We go to the continuum limit by letting $\epsilon \rightarrow 0$, $\Delta \rightarrow 0$, and $\Delta^2/\tau_0 \rightarrow \text{const}$. The resulting equation then has the following form:

$$\frac{\partial \langle h(x, t) \rangle}{\partial t} = \nu_2 \frac{\partial^2 \langle h(x, t) \rangle}{\partial x^2} - \nu_4 \frac{\partial^4 \langle h(x, t) \rangle}{\partial x^4} + \frac{\lambda}{2} \frac{\partial^2}{\partial x^2} \left\langle \left[\frac{\partial h(x, t)}{\partial x} \right]^2 \right\rangle + \dots \quad (10)$$

where the coefficients ν_2 , ν_4 , and λ depend on the functional form of the transition probabilities $W(i, i+1)$ and on the smoothing process. In general, there is also an infinite sequence of terms which are of higher order either in h or in the number of derivatives with respect to x .

(4) Equation (10) is assumed to be derivable from a Langevin equation by averaging over the noise. It follows then that this Langevin equation has the form

$$\frac{\partial h(x, t)}{\partial t} = \nu_2 \frac{\partial^2 h(x, t)}{\partial x^2} - \nu_4 \frac{\partial^4 h(x, t)}{\partial x^4} + \frac{\lambda}{2} \frac{\partial^2}{\partial x^2} \left[\frac{\partial h(x, t)}{\partial x} \right]^2 + \eta(x, t), \quad (11)$$

where the noise function $\eta(x, t)$ must be consistent with the conservation laws of the system, i.e., η is given by Eqs. (4). We have dropped the infinite sequence of other terms, which are, in principle, present in Eq. (10). These can be shown, by power counting, to be irrelevant in the renormalization-group sense if the noise function $\eta(x, t)$ is conservative.

Thus, steps (1)–(4) of the above argument led us to the conserved KPZ equation with an extra Laplacian term. In what follows we interpret our Monte Carlo results in terms of this equation.

We begin the discussion of possible surface structures emerging from Eq. (11) by considering the case when the dynamics obey detailed balance. Then the transition probability $W(i, i+1)$ is related to the change $\Delta H(i, i+1)$ of a potential function H when a particle is moved from site i to $i+1$. If we assume that this potential depends only on the slope of the interface, i.e., $H = J \sum_i f(\sigma_i)$ with $\sigma_i = (h_i - h_{i-1})/\epsilon$, which is reasonable for conserved dynamics when the movement of the particles is confined to the interface,²¹ then the potential is invariant under the combined transformation $\{h_i\} \rightarrow \{-h_i\}$ and $\{h_{i+j}\} \rightarrow \{h_{i-j+1}\}$. Therefore, the corresponding Langevin equation must be invariant un-

der the transformation $h(x, t) \rightarrow -h(x, t)$ and $x \rightarrow -x$. This excludes a term of the form $\partial_x^2 (\partial_x h)^2$ and, consequently, $\lambda = 0$ in eq. (11). Further details are given in the Appendix.

In the special case when H is a quadratic function of the slope of the interface

$$H = J \sum_i \left[\frac{h_i - h_{i-1}}{\epsilon} \right]^2, \quad (12)$$

one can show that the Laplacian term also disappears from Eq. (11) and thus one obtains

$$\frac{\partial h(x, t)}{\partial t} = -\nu_4 \frac{\partial^4 h(x, t)}{\partial x^4} + \eta(x, t). \quad (13)$$

This equation yields the scaling form (1) for the width of the surface with exponents $\chi = \frac{1}{2}$ and $z = 4$. As we shall see in Sec. III, procedure (i) and various generalizations of it that satisfy detailed balance all have exponents $\chi = \frac{1}{2}$ and $z = 4$. This is a somewhat puzzling result since it is not obvious that detailed balance would automatically produce a quadratic potential (12) and thus would exclude the Laplacian term in Eq. (11). A possible argument for $\nu_2 = 0$ in (11) can, however, be given as follows. Assume that the continuum limit of H exists:

$$H = \int d^d x \hat{f}(\nabla h) \quad (14)$$

and that, furthermore, the dynamics can be described by a Langevin equation that conserves the total height. Then the simplest model that one can write down is model B in critical dynamics:²²

$$\frac{\partial h}{\partial t} = -\nabla^2 \frac{\delta H}{\delta h} + \eta. \quad (15)$$

A straightforward substitution of (14) into (15) then shows that the Laplacian term does not appear in the Langevin equation.

The more general equation (11), which applies to the case in which detailed balance is broken, is more interesting. In this situation, the coefficients ν_2 , ν_4 , and λ are all finite and the scaling behavior resulting from this equation depends crucially on the sign of the coefficient ν_2 . Following are three distinct régimes.

(a) $\nu_2 > 0$. In this case, the term proportional to ν_4 is irrelevant, as is the nonlinear term. Since the Fourier transform of the noise function is proportional to k^2 for small k , the structure factor in the steady state does not diverge at long wavelength, and the surface is in fact flat ($\chi = 0$). The dynamic exponent z is equal to 2.

(b) $\nu_2 = 0$. This is a special case as far as Eq. (11) is concerned but may be rather common for discrete models even if they violate detailed balance. For example, in the conserved version of the single-step model,⁶ the master-equation approach described above yields explicit values for the coefficients ν_j and λ , and due to a symmetry that we do not fully understand, $\nu_2 = 0$, whether or not detailed balance is broken. With $\nu_2 = 0$, Eq. (8) becomes the one-dimensional version of the conserved KPZ equation [Eq. (2)], and the renormalization-group analysis of Sun, Guo, and Grant¹⁷ applies. The predicted exponents are

$\chi = \frac{1}{3}$ and $z = 4 - \chi$.

(c) $\nu_2 < 0$. Less is known about the solutions of Eq. (11) in this regime than for the previous two cases. In the noise-free case, there are a number of particular solutions for the steady-state profile. The one that seems to correspond most closely to the simulations reported below is a roof-top-like shape with period L . This phase with $\xi \sim L$ ($\chi = 1$) will be called the grooved phase henceforth. We note that similar equations with $\nu_2 < 0$ have been discussed recently by a number of authors.^{23,24} These authors, however, considered deposition processes, and consequently the particle conservation law is not present in their models.

III. MONTE CARLO SIMULATIONS

We have carried out extensive simulations for a number of variants of the models described in Sec. II. For example, one can consider a conserved version of the single-step model.⁶ In this model, $h_i - h_{i-1} = \pm 1$ at all times. The block size Δ is 2 for this model. The conserved version of the Kim and Kosterlitz model⁹ differs from this model by allowing $h_i - h_{i-1}$ to be zero as well and by the size of the blocks ($\Delta = 1$). We will report only representative results for the two important categories, namely models that obey detailed balance [procedure (i)] and for those that do not [procedure (ii)].

(i) *Surface diffusion with detailed balance.* We consider blocks of size $\Delta = 1$ and allow height differences between neighboring sites up to a maximum value $H = 1$. Since the dynamic exponent in this case is expected to be $z = 4$, if the arguments leading to Eq. (13) are correct, the number of Monte Carlo steps per site needed to achieve the steady state scales as L^4 . This makes it impossible to carry out simulations for very large substrates. Nevertheless, finite-size effects are not very strong, and we are confident that we have reached the thermodynamic limit.

This confidence is also supported by the following exact calculation of the steady-state value of ξ^2 . Since detailed balance is satisfied and since the transition rate is the same between any pair of states, which can be obtained from each other by a single hop of a particle, one concludes that all possible states are equally probable in the steady state. The calculation then proceeds as described in Ref. 6 with the conclusion that

$$\xi^2(t = \infty) = \frac{L+1}{18} \Delta^2. \quad (16)$$

In Table I we list the numerical values of the square of the steady-state width together with the values predicted from Eq. (16) for $L \leq 160$. The agreement is excellent.

In previous work^{2,6,8} we have shown that the steady-state exponent χ can be determined accurately from the small- k behavior of the structure factor $S(k)$ given by

$$S(k, t) = \frac{1}{L} \left\langle \sum_{m,j} h_m(t) h_j(t) e^{ik(m-j)} \right\rangle. \quad (17)$$

The width ξ is related to the structure factor through

$$\xi^2(L, t) = \frac{1}{L} \sum_k S(k, t) \approx \frac{1}{\pi} \int_{2\pi/L}^{\pi} dk S(k, t). \quad (18)$$

TABLE I. The square of the steady-state width of the model with $\Delta/H = 1$ and with dynamics that obey detailed balance [procedure (i)]. The effective exponent $\chi_{\text{eff}}(L)$ is defined in Eq. (19).

L	$\xi^2(L, \infty)$ Simulations	$\xi^2(L, \infty)$ Eq. (16)	$\chi_{\text{eff}}(L)$
10	0.581	0.611	
20	1.14	1.167	0.486
40	2.27	2.278	0.497
80	4.48	4.500	0.490
160	8.89	8.944	0.494

The divergence of the width is due to the divergence of the structure factor for small k . If $S(k) \sim k^{-2+\eta}$, the width diverges as $L^{(1-\eta)/2}$. Thus $\chi = (1-\eta)/2$. In Fig. 4 we show a log-log plot of the steady-state structure factor for systems of size $L \leq 160$. The straight line drawn through the small- k data points corresponds to $\eta = 0$. Thus we conclude that $\chi = 0.5$, consistent with the predictions of Eq. (13).

In Fig. 5 we show the relaxation of the interfacial width toward its steady-state value for short times and for a number of values of L as a function of the scaled variable tL^{-4} . The data collapse rather well to a single universal curve, even for rather small values of L , supporting the conclusion that this model is in the free-field universality class.

We have also simulated the same model with $\Delta = \frac{1}{2}$ and $\frac{1}{3}$ and the conserved single-step model with detailed balance. In all cases the results are consistent with those reported above.

(ii) *Models without detailed balance.* We now discuss the simulations for procedure (ii). As in the previous case, we have carried out the simulations for several versions of the basic model. We report here on the results for various ratios Δ/H , which turn out to be a control

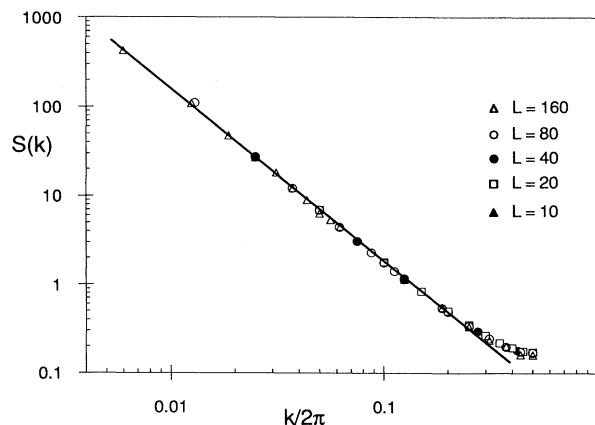


FIG. 4. The steady-state structure factor $S(k)$ [Eq. (17)] for procedure (i). The straight line has a slope 2, supporting the conclusion that $\chi = 0.5$.

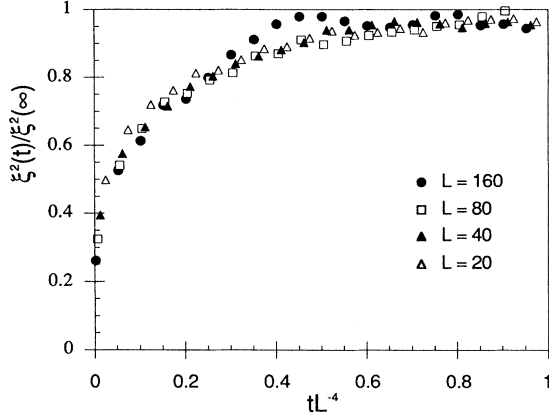


FIG. 5. The relaxation function for procedure (i). The data support the conclusion that $z=4$.

parameter that affects the coefficient v_2 in the phenomenological equation (11). The system is always initialized in the flat state. Blocks of size Δ are then moved from a randomly selected site to a nearest or next-nearest neighbor subject to the constraint that $|h_i - h_{i+1}| < H$ at all times. As described in Sec. II, if an attempted move in one direction fails, we attempt to move the block in the opposite direction. It is clear from the constraint $|h_i - h_{i+1}| \leq H$ that, for a given random-number sequence, the sequence of allowed moves will be identical for all ratios Δ/H in the range $1/n > \Delta/H > 1/(n+1)$. Thus the exponents χ and z can change only at these rational numbers of the control parameter Δ/H .

(a) $\Delta/H > \frac{1}{3}$. In Fig. 6 we have plotted the structure factor $S(k, \infty)$ for $\Delta/H=0.49$. It is clear that, rather than diverging at small k , $S(k, \infty)$ saturates. Thus, instead of diverging as $L \rightarrow \infty$, the width will reach a finite value. This conclusion is supported by the data for $\xi^2(L, \infty)$ in Table II for $L \leq 160$, where we have also given the values of the effective exponent

$$\chi_{\text{eff}}(L) = \frac{\ln[\xi^2(L)/\xi^2(L/2)]}{\ln(2)}. \quad (19)$$

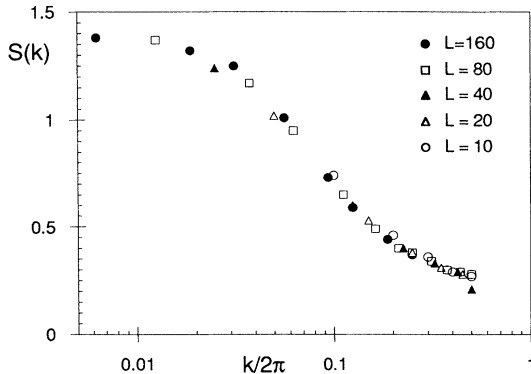


FIG. 6. The steady-state structure factor for procedure (ii) for $\Delta/H=0.49$.

TABLE II. The same as Table I for the model with $\Delta/H=0.49$ and with dynamics that do not obey detailed balance [procedure (ii)].

L	$\xi^2(L, \infty)$	$\chi_{\text{eff}}(L)$
10	0.451	
20	0.614	0.22
40	0.755	0.15
80	0.828	0.067
160	0.868	0.034

It is clear that this exponent is rapidly approaching zero as the system size increases.

The dynamic exponent z is difficult to determine from the short-time behavior of the width. Since there is no long-wavelength divergence of the structure factor, all modes are equally important, and finite-size effects play an important role. We have determined an effective dynamic exponent $z_{\text{eff}}(L)$ by examining the relaxation of the time-dependent structure factor $S(k, t)$ for the smallest wave vectors. Specifically, we vary z to obtain the best possible collapse of the data for the function

$$\Psi(k, t) = 1 - \frac{S(k, t)}{S(k, \infty)} \quad (20)$$

when plotted as a function of $k^z t$ for the five smallest wave vectors for a given value of L . The value that produces the best fit is $z_{\text{eff}}(L)$. The values are $z_{\text{eff}}(40)=2.85$, $z_{\text{eff}}(80)=2.5$, and $z_{\text{eff}}(160)=2.3$. These results are consistent with an extrapolated value $z = z_{\text{eff}}(\infty) = 2.0$.

The behavior of the steady-state structure factor and relaxation function (20) indicates that the appropriate continuum equation for this value of Δ/H is Eq. (11) with $v_2 > 0$. This implies that the other terms in this equation are irrelevant in the renormalization-group sense although they will in general be present and contribute to the rather pronounced finite-size effects.

(b) $\Delta/H = \frac{1}{3}$. In Fig. 7 we display the steady-state structure factor for this case for systems of size up to

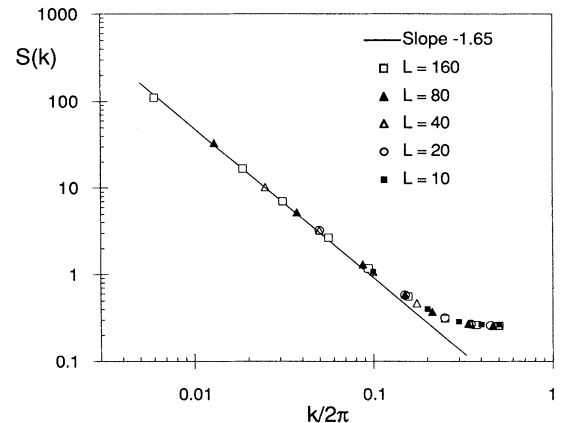


FIG. 7. Same as Fig. 6 but for $\Delta/H = \frac{1}{3}$.

$L=160$. In contrast to the previous case the structure factor now shows a clear power-law divergence for small k . The straight line, which provides an excellent fit to the data over at least half the Brillouin zone, has slope -1.65 , which indicates that $\chi \approx 0.35$. The data for the equilibrium width are consistent with this conclusion.

Figure 8 shows the relaxation of the width of the interface to its steady-state value plotted as a function of the scaled time tL^{-z} with $z=3.67$. The collapse of the data is very good and, although there is an uncertainty of order 0.1 in the estimate of z , the value of 4.0 that we obtained for the case of procedure (i) is clearly ruled out at least for systems of this size.

The exponents $z \approx \frac{11}{3}$ and $\chi \approx \frac{1}{3}$ as well as the scaling law $z + \chi = 4$, which the data support, lead us to conjecture that at $\Delta/H = \frac{1}{3}$ is a critical point of the model where the coefficient ν_2 in Eq. (11) vanishes. As was shown in Ref. 17, the nonlinear term is then relevant for substrate dimensions less than 2. The renormalization-group treatment of the continuum equation then produces the exponents $z = \frac{11}{3}$ and $\chi = \frac{1}{3}$ to first order in an ϵ expansion about the critical dimension $d_c = 2$.

(c) $\Delta/H < \frac{1}{3}$. The entire regime $\Delta/H < \frac{1}{3}$ can be characterized as a grooved phase in which the width of the surface is proportional to the length of the substrate. However, the asymptotic behavior of the system sets in at smaller and smaller values of L as Δ/H becomes smaller. Here we will report only the results for $\Delta/H = \frac{1}{40}$. For this case one can see the onset of the asymptotic behavior for systems as small as $L = 80$.

In Table III we list the steady-state value of the mean-square width for systems up to size $L = 240$ together with the effective exponent defined in Eq. (19). In contrast to the flat phase and the critical phase, the width of the surface in this phase increases very rapidly as a function of L . For example, for $L = 160$, the steady-state value of ξ^2 for $\Delta/H = \frac{1}{40}$ is more than 200 times as large as that for $\Delta/H = 0.33$. Indeed, the effective exponent χ_{eff} is larger than 1.0 for all values of L as shown in Table III. This is already an indication that we have not reached the

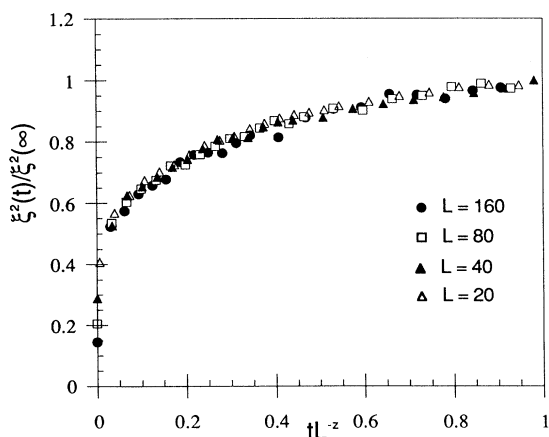


FIG. 8. Relaxation function for procedure (ii) with $\Delta/H = \frac{1}{3}$. The data are plotted as function of tL^{-z} with $z = 3.67$.

TABLE III. The same as Table I for the model with $\Delta/H = \frac{1}{40}$ and with dynamics that do not obey detailed balance [procedure (ii)].

L	$\xi^2(L, \infty)$	$\chi_{\text{eff}}(L)$
10	0.424	
20	2.01	1.12
40	19.2	1.63
80	128.3	1.37
160	634.4	1.15
240	1501.0	1.06

asymptotic regime in these simulations since $\chi \leq 1$ for any system for which the slope of the surface is bounded (in this case by H). As shown in Table III, the effective exponent attains a maximum as a function of L and then decreases toward a limiting value which we believe to be exactly 1.0. This behavior is generic in the grooved phase; only the turning point varies with Δ/H , appearing at decreasing values of L as Δ/H is decreased.

The average shape of the surface in the grooved phase (Fig. 9) appears to be the deterministic (noise-free) steady-state solution of the conserved KPZ equation (3):

$$h(x) = h_0 - \frac{2}{\lambda} \ln \left\{ \cosh \left[\left(\frac{\lambda b}{2} \right)^{1/2} (x - x_0) \right] \right\}. \quad (21)$$

Here x_0 and h_0 are chosen to fit the position and value of the maximum height of the surface, while λ and b can be used to fit both the curvature at the maximum and the maximal height difference. Figure 9 shows a comparison of a typical steady-state Monte Carlo configuration for $\Delta/H = \frac{1}{40}$ with Eq. (21). The quality of the fit is similar in the entire range $\Delta/H < \frac{1}{4}$.

There are two problems with the solution (21). The first is that the conserved KPZ equation has another locally stable solution, namely $h(x) = 0$. A plausible resolution of this difficulty is that the diffusion coefficient ν_2 in

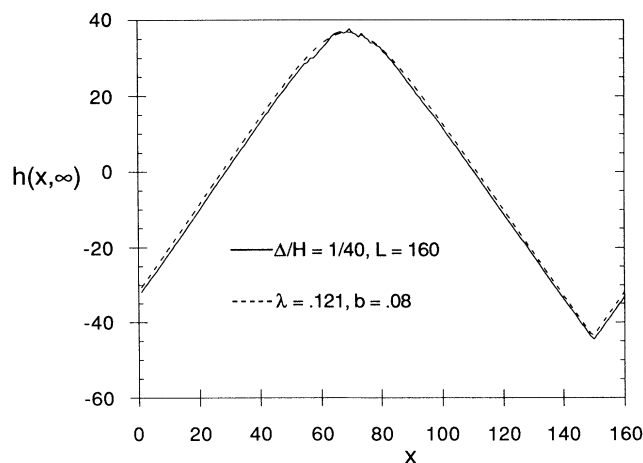


FIG. 9. Typical steady-state configuration of the interface for $\Delta/H = \frac{1}{40}$ (solid curve) and fit to Eq. (21) (dashed curve).

Eq. (11) is positive for $\Delta/H = \frac{1}{2}$, zero for $\Delta/H = \frac{1}{3}$. Thus by continuity one expects it to be negative for $\Delta/H < \frac{1}{4}$. The change of sign in ν_2 then provides the instability mechanism that destabilizes the solution $h(x)=0$, and the shape of the surface is actually given by the solution of Eq. (11) with a small negative ν_2 .

The second problem with (21) is the lack of periodicity. One can, however, construct periodic solutions by pasting together solutions of the form (21) shifted by kL , where k is an integer and where the shifted function gives the solution in the range $kL \leq (x - x_0) \leq (k+1)L$. The bottoms of the grooves then become singular points at which the slope of the surface changes from $-q$ to q with $q \sim O(1)$. It should be noted, however, that the differential equation that governs the steady-state shape contains only $(\partial h / \partial x)^2$ and even derivatives of h . Thus all the quantities that appear in the differential equation are continuous functions at the singular points. (Note that if we consider functions that are symmetric about the point x_0 , then the functions are symmetric about the points where the solutions are pasted together as well.)

Thus we believe that Eq. (11) with a small negative ν_2 describes the steady-state shape of the surface for $\Delta/H \leq \frac{1}{4}$. We do not, however, have a ready explanation for the fact that (21) gives an excellent fit to the data in the entire range $\Delta/H \leq \frac{1}{4}$, thus implying that ν_2 remains very small in that entire range. It is, of course, a possibility that $\nu_2=0$ for $\Delta/H \leq \frac{1}{4}$ and that the loss of stability of the solution $h(x)=0$ of the conserved KPZ equation is due to some nonlinear term not accounted for in Eq. (11).

The relaxation towards the steady state seems to be an activated process and does not show scaling behavior. Typically, for a system of size L , the width initially grows with a power-law dependence on t , similar to case (b). However, at some reasonably short time, of order L^4 , an instability develops, and the width rapidly shoots up to the steady-state value. We have, therefore, not found it useful to characterize the relaxation in terms of a scaling function.

If our conjecture that the grooved phase can be described by Eq. (11) with $\nu_2 < 0$ is correct, then we have a phase transition as a function of the control parameter Δ/H from the flat phase to this grooved phase. Precisely at the critical point $\Delta/H = \frac{1}{3}$ ($\nu_2=0$), the model displays nontrivial scaling and exponents consistent with the

renormalization-group predictions for Eq. (11). We note also that Eq. (11) has been discussed by Golubovic and Bruinsma²³ for the case of nonconserved noise, i.e., a growing deposit. They also make a point that negative ν_2 leads to an instability of a flat surface toward grooves and overhangs in systems where these are allowed.

We note also that the same transition from a flat to a grooved interface can also be seen as function of a continuous control parameter (rather than the rational values $\Delta/H = 1/n$). If one allows variable size blocks drawn from a distribution with a cutoff $\Delta_{\max} < H$, then Δ_{\max}/H plays the same role as Δ/H in the present simulations but can take on any value. We have done a few calculations for such a model and observed both flat and grooved phases, presumably separated by a critical point with the properties described in case (b).

In conclusion, we have shown that a simple model of surface dynamics exhibits a surprisingly rich phase diagram. The model in which the dynamics violate detailed balance displays a phase transition from a flat to a grooved phase. Precisely at the critical point, the model seems to be in the universality class of the conserved KPZ equation.

ACKNOWLEDGMENTS

We have benefited from conversations with Marcel den Nijs, Hans-Werner Diehl, Martin Grant, Hong Guo, Beate Schmittmann, and Royce Zia. This research was supported by the Natural Sciences and Engineering Research Council (NSERC) of Canada. M.S. acknowledges financial support by the Deutsche Forschungsgemeinschaft.

APPENDIX

We restrict ourselves to the case of transition probabilities [Eq. (8)] that exhibit left-right symmetry. The calculation can easily be generalized. Then the following relations hold:

$$\begin{aligned} W(i, i+1) &= \phi(\sigma_{i-1}, \sigma_i, \sigma_{i+1}, \sigma_{i+2}), \\ W(i+1, i) &= \phi(-\sigma_{i+3}, -\sigma_{i+2}, -\sigma_{i+1}, -\sigma_i). \end{aligned} \quad (\text{A1})$$

Expanding the right-hand side of (7) in powers of $(h_i - h_{i-1})/\epsilon$ results in the following expression:

$$\begin{aligned} \frac{\tau_0}{\Delta} \partial_t \langle h_i \rangle &= -2\epsilon(\phi_1 + \phi_2 + \phi_3 + \phi_4) \langle \partial_x^2 h_i \rangle - \frac{1}{6}\epsilon^3 [25\phi_1 + 7(\phi_2 + \phi_4) + \phi_3] \langle \partial_x^4 h_i \rangle \\ &+ \epsilon^2(2\phi_{11} + 3\phi_{12} + 2\phi_{13} + \phi_{14} + \phi_{22} - \phi_{44} + \phi_{23} - \phi_{34}) \langle \partial_x^2 (\partial_x h_i)^2 \rangle + O(\epsilon^3), \end{aligned} \quad (\text{A2})$$

where

$$\begin{aligned} \phi_i &= \left. \frac{\partial \phi(\xi_1, \xi_2, \xi_3, \xi_4)}{\partial \xi_i} \right|_{\xi=0}, \\ \phi_{ij} &= \left. \frac{\partial^2 \phi(\xi_1, \xi_2, \xi_3, \xi_4)}{\partial \xi_i \partial \xi_j} \right|_{\xi=0} \end{aligned} \quad (\text{A3})$$

and $\langle \partial_x^2 h_i \rangle$ denotes the discrete version of the second derivative, i.e.,

$$\langle \partial_x^2 h_i \rangle = \langle h_{i+1} - 2h_i + h_{i-1} \rangle / \epsilon^2.$$

The other derivatives are defined analogously. When detailed balance holds, derivatives of ϕ with respect to the

first argument vanish, i.e., $\phi_1=0$ and $\phi_{1,j}=0$, $j=1, \dots, 4$, and we have the additional symmetry $\phi(\xi_2, \xi_3, \xi_4)=\phi(\xi_4, \xi_3, \xi_2)$. Therefore, $\phi_2=\phi_4$, and $\phi_{2j}=\phi_{4j}$ for $j=1, \dots, 4$. This results in the disappearance of the conserved KPZ term $\langle \partial_x^2 (\partial_x h_i)^2 \rangle$. The

coefficient $\phi_2+\phi_3+\phi_4$ is generally nonzero. In the detailed-balance case we believe, however, that this coefficient vanishes as a consequence of the coarse-graining process yielding a result consistent with our simulations of procedure (i).

*On leave from Institute for Theoretical Physics, Eötvös University, 1086 Budapest, Hungary.

¹F. Family and T. Vicsek, *J. Phys. A* **18**, L75 (1985).

²M. Plischke and Z. Rácz, *Phys. Rev. A* **32**, 3825 (1985).

³R. Jullien and R. Botet, *Phys. Rev. Lett.* **54**, 2055 (1985).

⁴F. Family, *J. Phys. A* **19**, L441 (1986).

⁵P. Meakin, P. Ramanlal, L. M. Sander, and R. C. Ball, *Phys. Rev. A* **34**, 5081 (1986).

⁶M. Plischke, D. Liu, and Z. Rácz, *Phys. Rev. B* **35**, 3485 (1987).

⁷D. E. Wolf and J. Kertesz, *Europhys. Lett.* **4**, 651 (1987).

⁸D. Liu and M. Plischke, *Phys. Rev. B* **38**, 4781 (1988).

⁹J. M. Kim and J. M. Kosterlitz, *Phys. Rev. Lett.* **62**, 2289 (1989).

¹⁰J. Krug, *J. Phys. A* **22**, L769 (1989).

¹¹J. G. Amar and F. Family, *Phys. Rev. Lett.* **64**, 543 (1990).

¹²Y. P. Pellegrini and R. Jullien, *Phys. Rev. Lett.* **64**, 1745 (1990).

¹³B. M. Forrest and L-H. Tang, *Phys. Rev. Lett.* **64**, 1405 (1990).

¹⁴M. Kardar, G. Parisi, and Y-C. Zhang, *Phys. Rev. Lett.* **56**, 889 (1986).

¹⁵J. Krug, *Phys. Rev. A* **36**, 5465 (1987).

¹⁶H. Guo, B. Grossmann, and M. Grant, *Phys. Rev. Lett.* **64**, 1262 (1990).

¹⁷T. Sun, H. Guo, and M. Grant, *Phys. Rev. A* **40**, 6763 (1989).

¹⁸A. Chakrabarti, *J. Phys. A* **23**, L919 (1990).

¹⁹H. Guo and M. Grant (private communication).

²⁰A. De Masi, P. A. Ferrari, and J. L. Lebowitz, *Phys. Rev. Lett.* **55**, 1947 (1985).

²¹It should be noted that this assumption does not exclude induced currents within the interface. These would be described by odd powers in the function $f(\sigma_i)$.

²²P. C. Hohenberg and B. I. Halperin, *Rev. Mod. Phys.* **49**, 435 (1977). Note that ∇^2 in Eq. (15) should, in principle, be replaced by a more general form that takes into account the fact that the particles move on an interface. The additional nonlinear terms do not, however, affect our conclusion that the Laplacian term is absent in (15).

²³L. Golubovic and R. Bruinsma, *Phys. Rev. Lett.* **66**, 321 (1991).

²⁴A. Mazar, D. J. Srolovitz, P. S. Hagan, and B. G. Bukiet, *Phys. Rev. Lett.* **60**, 424 (1988); J. Villain, *J. Phys. I (France)* **1**, 19 (1991).